MULTIPLE SCENE ATTITUDE ESTIMATOR PERFORMANCE FOR LANDSAT-1

Samuel S. Rifman, A. T. Monuki and C. P. Shortwell

TRW Defense and Space Systems Group

ABSTRACT

Initial results are presented to demonstrate the performance of a linear sequential estimator (Kalman Filter) used to estimate a LANDSAT-1 spacecraft attitude time series defined for four scenes. Previous work has shown that a similar estimator valid for one scene could facilitate precision geometric correction (rectification) and multitemporal registration to pixel (or better) accuracies. With the revised estimator a GCP poor scene – a scene with no usable geodetic control points (GCPs) – can be rectified to higher accuracies than otherwise, based on the use of GCPs in adjacent scenes. Attitude estimation errors have been determined by the use of GCPs located in the GCP-poor test scene, but which are not used to update the Kalman filter. Initial results achieved to date indicate that errors of <500m (rms) can be attained for the GCP-poor scenes. Operational factors are related to various scenarios.

1. INTRODUCTION

Since the launch of LANDSAT-1, much effort has been devoted to the development of digital methods for the geometric and radiometric correction of multispectral scanner (MSS) data collected by the LANDSAT series of spacecraft. As early as 1973 (References 1-3), examples of MSS data corrected to sub pixel accuracies by all digital methods were generated and reported on in the literature. Subsequent advances included scene/scene registration to sub pixel accuracies of multitemporal data (References 4,5).

A particularly successful technique employed to reduce the data processing load and yet achieve high accuracy entails the novel use of a linear sequential estimator (Kalman filter) for estimation of the satellite attitude state vector (Reference 6). Results have been previously reported regarding the evaluation by various methods of the estimator's accuracy for precision registration of full scene LANDSAT MSS data (Reference 4,5) and rectification of single scene data (References 1-3, 7).

In the previously referenced work, a given scene was corrected using knowledge of the spacecraft position, attitude and the sensor scan mechanism. For a given site* the locations of features within the imagery, referred to as contro points, were employed to refine estimates of the spacecraft attitude state vector defined for the same site. Registration was accomplished by means of essentially the same procedure, but with two small modifications: (a) measurement uncertainties were made much smaller than in the case of rectification (effectively giving less weight to a priori data); and (b) control points were used even if their precise geodetic locations on the earth's surface were unknown.

While it often is sufficient to employ a site specific estimator for rectification/registration purposes, the technique is dependent upon the availability of control points for the site in question. In some cases of interest, the subject site may have few or no usable geodetic control points (GCPs) the locations of which on the earth's surface are known to high accuracy. Examples of such cases include sites remote from civilization, sites containing featureless terrain, sites with poorly defined land/water interfaces, or sites which have not been surveyed to establish geodetic control.

*A site refers to a framed MSS scene approximately 185 km on a side.

In this paper, we report on the results of a technique which can increase the geometric correction and absolute location accuracy of such GCP poor sites when nearby sites do have adequate geodetic control. The technique is based essentially upon an extended definition of the attitude time series of the satellite, to encompass N sequential scenes in the direction of satellite motion.

It is not the purpose of this paper to present the details of the algorithm and design for the extended attitude estimator, per se. Rather it is the objective herein to present initial performance results of the estimator, and to identify certain features of the estimator's performance which may be of general interest.

2. PERFORMANCE EVALUATION METHOD

Based on available data for the LANDSAT attitude control system and attitude measurement system (Reference 8), as well as experience derived from previous work with the single scene estimator (References 6 and 7), it was decided to configure an initial series of tests involving four sequential LANDSAT scenes. Table 1 lists the scenes employed for this purpose, derived from path 16 of the Worldwide Reference System. There were 20 geodetic control points (GCPs) available per each scene, and the GCPs were approximately uniformly distributed within each scene.

The evaluation procedure proceded in two steps. First, for a given scenario, the m scenes (one, two or three in number) which were GCP poor were identified. The GCPs from the GCP poor scenes were not used to update the attitude estimator (they are, in fact, the statistical control points of Reference 7). Estimation errors were computed at the GCPs of the GCP poor sites, based upon updates of the estimator by means of GCP location data in the GCP rich sites (4-m in number).

The second step of the evaluation procedure reported on herein entailed calculation of the estimation errors at the GCPs of the GCP poor sites based only on a priori SIAT data recorded on the Computer Compatible Tapes purchased from the EROS Data Center.* The SIAT data includes attitude, altitude and sub-point position of the satellite for approximately 10 points in time spanning each 185Km x 185Km framed scene.

A relative comparison of the estimation errors obtained from the two steps of evaluation was the basis for determination of the improvement in attitude estimation accuracy achieved with the multiple scene attitude estimator, in contrast to performance achievable without the use of any GCPs from the site in question. This evaluation was undertaken for various scenarios of GCP rich/GCP poor scenes. Table 2 lists the various scenarios evaluated herein.

Upon commencing the evaluations, it was determined that the SIAT attitude data for successive scenes was discontinuous. Figure 1 shows the roll data for a sequence of scenes obtained directly from a NASA-produced Bulk Image Anno-

*SIAT data for a number of scenes is contained on a Bulk Image Annotation Tape (BIAT). The scene CCTs employed for the initial evaluations were obtained before SIAT data was recorded on CCTs. Thus, it was necessary in this study to employ the NASA BIAT tape data, which subsumes the currently provided SIAT data.

TABLE 1. LANDSAT-1 Scenes Employed for Multiscene Analysis

Scene Number	Scene ID Number	Row Number	Number of GCPs Available
1	1080-15183	31	20
2	1080-15185	32	20
3	1080-15192	33	20
4	1080-15194	34	20

TABLE 2. Scenarios Used for Performance Evaluation

Scenario Number	Scene ID Number 1080-15183	1080-15185	1080-15192	1080-15194
1	1	0	1	*
2	1	0	*	1
3	1	*	0	1
4	1	0	1	1
5	1	1	0	1
6	1	0	*	*
7	1	*	0	*
8	1	*	*	0
9	1	1	0	*
10	1	1	*	0
11	1	1	1	0

*: Scene not utilized
0: GCP poor scene
1: GCP rich scene

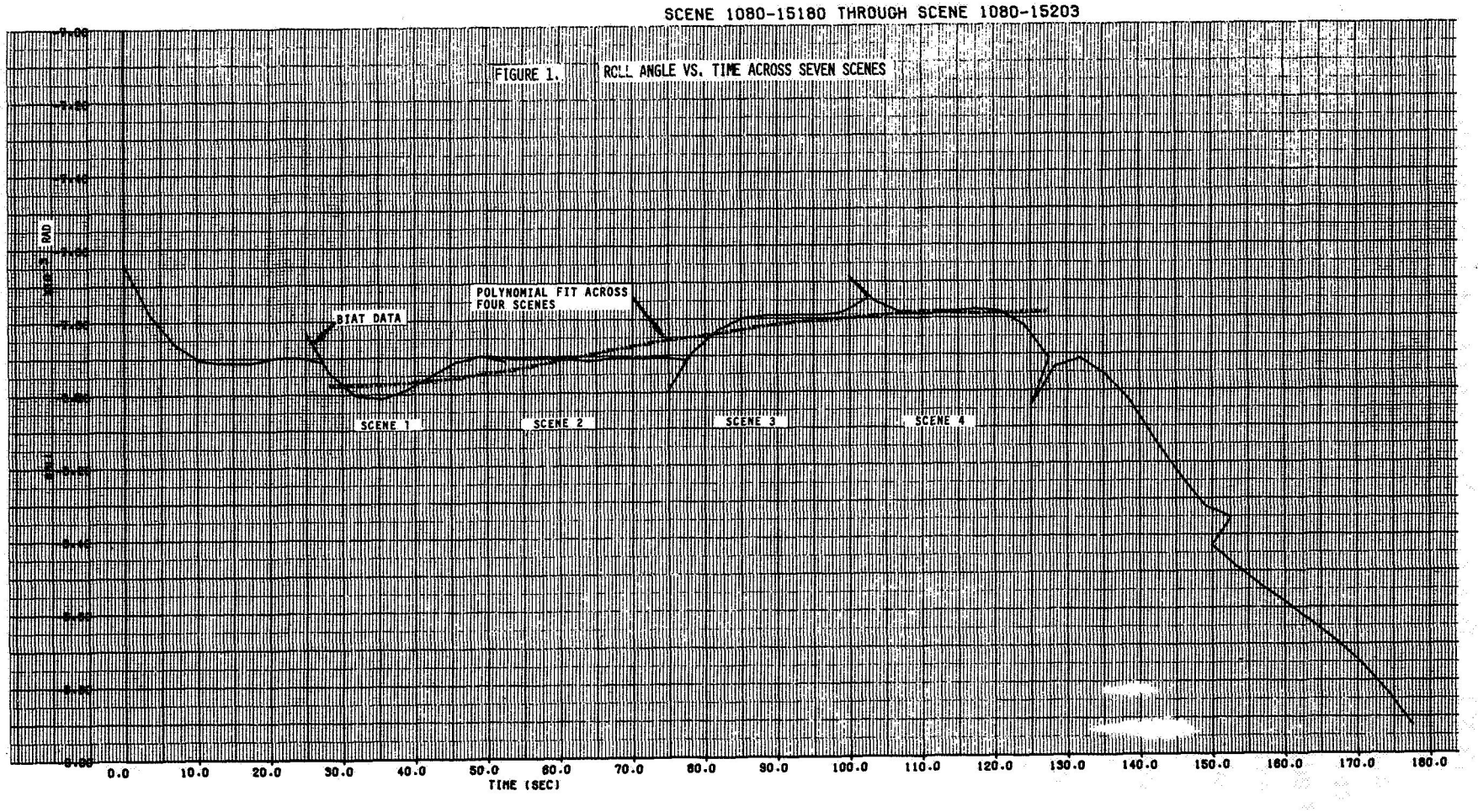
SCENE 1080-15180 THROUGH SCENE 1080-15203
FIGURE 1. ROLL ANGLE VS. TIME ACROSS SEVEN SCENES
POLYNOMIAL FIT ACROSS FOUR SCENES
BIAT DATA
SCENE 1
SCENE 2
SCENE 3
SCENE 4
TIME (SEC)
0.0
10.0
20.0
30.0
40.0
50.0
60.0
70.0
80.0
90.0
100.0
110.0
120.0
130.0
140.0
150.0
160.0
170.0
180.0

Figure 1

tation Tape (BIAT). It appears from a study of this and other such data that the SIAT attitude data is the result of a cubic time series fit to processed telemetry data for attitude, and that the fit is performed on a single scene basis; hence, there is a discontinuity in attitude in the overlap region of two framed adjacent along track MSS scenes.

In order to initialize the multiple scene attitude estimator, a global cubic attitude time series was fit to the aforesaid attitude data obtained from the BIAT. Selected BIAT data in the overlap regions were disregarded in order to achieve a good least squares fit to what appeared to be the underlying attitude data*. Figure 1 also shows the fit data in relation to the BIAT data. The resultant fit errors are shown in Table 3.

GCPs were employed alternately from the GCP rich scenes, to update the estimator. That is, one GCP was employed from the first GCP rich scene, and then another from the second such scene, until the last GCP had been processed. This method was employed to avoid biasing the global time series on the basis of only one GCP rich scene in the sequence. With each GCP update the estimation errors at the statistical control points (GCPs in the GCP poor scenes which do not update the estimator) were evaluated. The errors at each statistical control point (SCP) were evaluated. The error at each statistical control point was computed as the along track, across track and altitude components of the vector difference in earth centered rotating coordinates of the known statistical control point position and the estimated position for the same control point. The estimated control point position was computed on the basis of the previous attitude state vector (resulting from the previous update of the state vector by GCP location data in one of the GCP rich scenes) and the location of the control point feature within the image. The control points are located to $\pm 1/8$ pixel accuracy by a manual control point designation process. This process employs 4:1 digital enlargement by cubic convolution resampling (Reference 9) of a control point feature displayed on an interactive image display system.

---

*Processed attitude data, before polynomial model fitting, could not be obtained.

TABLE 3. Fit Errors over 4 Scenes 1, 2, 3, 4

	Roll	Pitch	Yaw
Maximum Error	0.06 mr (54 m)	.21 mr (190 m)	.065 mr (6 m)
RMS Error	.03 mr (27 m)	.108 mr (97 m)	.035 mr (3.2 m)

3. RESULTS

The results for two types of scenarios are presented. The first type of scenario corresponds to the case in which one or more GCP poor scenes lie between two or more GCP rich scenes. This interpolation scenario contrasts to the extrapolation scenario, in which one or more GCP poor scenes precede or follow one or more GCP rich scenes.

A. Interpolation Results

Interpolation results are listed in Table 4 for the scenarios identified by scene in Table 1. The Bulk Error corresponds to rms errors (meters) measured at GCPs which do not update the estimator (SCPs), on the basis of the NASA BIAT attitude defined for the individual GCP poor scene of each scenario.

A Priori Error is the rms estimation error (meters) measured at the SCPs in the GCP poor scene of each scenario, on the basis of the smooth global attitude time series (single cubic time series spanning 4 scenes). The remaining two columns are the a posteriori estimation errors for all the GCP rich scenes, and the GCP poor scene of each scenario.

A total of 10 GCPs were employed, regardless of the number of GCP rich scenes. It was found that the estimator converged rapidly with no more than 10 GCP updates.

Comparison of the Bulk Error data to the A Posteriori Error for the same GCP poor scene is a direct measure of the efficacy of the global attitude estimator in comparison with processing such scenes in the absence of GCPs (in said scenes). The scene errors are dramatically reduced in all cases. There is a small remaining altitude component of error, but along track errors are reduced to 60% of the Bulk Error and across track errors are reduced typically to 50% of the corresponding Bulk Error values.

B. Extrapolation Results

Extrapolation results are presented in Table 5 for the scenarios identified by scene in Table 1. In this case, not all scenarios exhibit improved performance, and those with non-contiguous single GCP rich/poor scenes are distinctly worse off than the corresponding Bulk Errors. Contiguous single GCP rich/poor scenes are improved somewhat and significant performance improvement is achieved with two or more contiguous GCP rich scenes contiguous with a GCP poor scene.

TABLE 4. Interpolation Results

Scenario	Bulk Error (M, RMS) Over GCP Poor Scene	A Priori Error (M, RMS) Over GCP Poor Scene	A Posteriori Error (M, RMS) Over GCP Rich Scenes	A Posteriori Error (M, RMS) Over GCP Poor Scene
101*	AT 759	900	49	418
	CT 556	661	63	266
	H 30	30	33	35
10*1	AT 759	900	58	401
	CT 556	661	54	320
	H 30	30	33	36
1*01	AT 1057	947	58	414
	CT 582	577	58	135
	H 36	33	33	38
1011	AT 759	900	93	481
	CT 556	661	74	276
	H 30	30	33	34
1101	AT 1057	1050	45	603
	CT 582	591	87	98
	H 36	31	36	36

AT = Along Track
CT = Cross Track
H = Altitude

* Scene Not Utilized
0 GCP Poor Scene
1 GCP Rich Scene

TABLE 5. Extrapolation Results

Scenario	Bulk Error (M, RMS) Over GCP Poor Scene	A Priori Error (M, RMS) Over GCP Poor Scene	A Posteriori Error (M, RMS) Over GCP Rich Scenes	A Posteriori Error (M, RMS) Over GCP Poor Scene
10**	AT 759	900	87	600
	CT 556	661	55	408
	H 30	30	39	37
1*0*	AT 1057	1050	87	1532
	CT 582	591	55	522
	H 36	31	39	41
1**0	AT 907	684	87	1562
	CT 631	579	55	728
	H 42	29	39	39
110*	AT 1057	1050	49	614
	CT 582	591	92	86
	H 36	31	36	36
11*0	AT 907	684	34	697
	CT 631	579	90	182
	H 42	29	34	35
1110	AT 907	684	53	594
	CT 631	579	65	140
	H 42	29	39	34

AT = Along Track
CT = Cross Track
H = Altitude

* Scene Not Utilized
0 GCP Poor Scene
1 GCP Rich Scene

4. CONCLUSIONS

In general, it was found that interpolation mode error statistics were stable, that is, not sensitive to GCP processing order or location error of the GCPs. On the other hand, the extrapolation mode tended to be relatively less stable if extrapolated from one GCP rich scene. Not unexpectedly, performance deteriorates with separation of GCP rich and poor scenes in the extrapolation mode. However, extrapolation with two or more GCP rich scenes significantly increases stability and accuracy.

Clearly, more work needs to be done to examine the effects of attitude modeling errors, number of scenes which can be processed and the distribution of GCPs. Nonetheless, a significant improvement in geometric accuracy performance for scenes without GCPs can be expected with the use of a global state vector updated by GCPs in nearby sites.

REFERENCES

1. S. S. Rifman, "Digital Rectification of ERTS Multispectral Imagery," Symposium on Significant Results Obtained from the Earth Resources Technology Satellite-1, New Carrolton, Md., NASA SP-327, p. 1131 (March 5-9, 1973).

2. S. S. Rifman, "Evaluation of Digitally Corrected ERTS Imagery," Symposium on Management and Utilization of Remote Sensing Data, Sioux Falls, South Dakota, p. 284 (Obtober 29-November 1, 1973).

3. J. E. Taber, "Evaluation of Digitally Corrected Images," Third Earth Resources Technology Satellite-1 Symposium, Washington, D.C., NASA SP-351, p. 1837 (December 10-14, 1973).

4. R. H. Caron, "Evaluation of Full-Scene Registered ERTS MSS Imagery Using a Multitemporal/Multispectral Bayes Supervised Classifier," Fourth Annual Remote Sensing of Earth Resources Conferences, University of Tennessee Space Institude, Tullahoma, Tennessee (March, 1975).

5. S. S. Rifman, et al., "Second Generation Digital Techniques for Processing LANDSAT MSS Data," Earth Resources Survey Symposium, Houston, Texas (June 8-12, 1975).

6. R. H. Caron and K. W. Simon, "Attitude Time-Series Estimator for Rectification of Spaceborne Imagery," Journal of Spacecraft and Rockets 12, 27 (January 1975).

7. S. S. Rifman and W. B. Allendoerfer, "LANDSAT MSS Rectification and Registration Results Obtained by Using a Precision Attitude Estimator," paper present to The Flight Mechanics/Estimation Theory Symposium, NASA, Greenbelt, Maryland (October 29-30, 1975).

8. LANDSAT Data Users Handbook, NASA Document No. 76SDS4258 (September 2, 1976).

9. K. W. Simon, "Digital Image Reconstruction and Resampling for Geometric Manipulation," Symposium on Machine Processing of Remotely Sensed Data, West Layfayette, Indiana (June 3-5, 1975).